Journal of Alloys and Compounds 512 (2012) 63–67

Contents lists available at SciVerse ScienceDirect

Journal of Alloys and Compounds

journal homepage: www.elsevier.com/locate/jallcom

Densification and mechanical properties of fine-grained Al_2O_3–ZrO_2 composites consolidated by spark plasma sintering

Fancheng Meng[a], Cheng Liu[a], Fan Zhang[b], Zhongqing Tian[a], Weijiu Huang[a,*]

[a] Department of Materials, Chongqing University of Technology, Chongqing 400054, China
[b] State Key Lab of Advanced Technology for Materials Synthesis and Processing, Wuhan University of Technology, Wuhan 430070, China

ARTICLE INFO

Article history:
Received 31 December 2010
Received in revised form 26 August 2011
Accepted 4 September 2011
Available online 10 September 2011

Keywords:
Microstructure
Mechanical property
Al_2O_3
Spark plasma sintering

ABSTRACT

Alumina matrix composites containing 5 and 10 wt% of ZrO_2 were sintered under 100 MPa pressure by spark plasma sintering process. Alumina powder with an average particle size of 600 nm and yttria-stabilized zirconia with 16 at% of Y_2O_3 and with a particle size of 40 nm were used as starting materials. The influence of ZrO_2 content and sintering temperature on microstructures and mechanical properties of the composites were investigated. All samples could be fully densified at a temperature lower than 1400 °C. The microstructure analysis indicated that the alumina grains had no significant growth (alumina size controlled in submicron level 0.66–0.79 μm), indicating that the zirconia particles provided a hindering effect on the grain growth of alumina. Vickers hardness and fracture toughness of composites increased with increasing ZrO_2 content, and the samples containing 10 wt% of ZrO_2 had the highest Vickers hardness of 18 GPa (5 kg load) and fracture toughness of 5.1 MPa $m^{1/2}$.

1. Introduction

Due to exhibiting high hardness, strength and fracture toughness, Al_2O_3–ZrO_2 composites have been widely used for various applications such as cutting-tools, biomedical implants and structural parts. Especially, in orthopedics, they exhibit a larger crack resistance than alumina and a lower sensitivity for aging than zirconia [1–3].

Recent studies suggested that the mechanical properties of Al_2O_3–ZrO_2 composites could have a considerable increase by reducing their grain size and increasing their dispersivity. Al_2O_3–ZrO_2 composites with high transformation toughening can be obtained if a high portion of tetragonal phase with the ability to transform under applied stress is retained at room temperature [4,5]. To meet this requirement, the size of zirconia grain must be lower than a critical size (0.7 μm) to ensure the stable of tetragonal phase at room temperature [6–8]. A fine-grained matrix Al_2O_3 also results in an enhanced mechanical property. Furthermore, it is suggested that a smaller matrix size (grain at submicron level or nanoscale) will result in a higher improvement in mechanical property. Therefore, dense fine-grained Al_2O_3–ZrO_2 composites are desirable to be achieved [7–9]. Unfortunately, it is difficult to obtain Al_2O_3–ZrO_2 composites with high density and smaller grain size. This is mainly due to the inevitable grain growth during the sintering process. In addition, the low heating rate used in a conventional sintering requires a long heating duration from room temperature to the target sintering temperature, which resulting in the coarseness of the nanoparticles [10]. To minimize grain growth, unconventional sintering and densification methods have been proposed. Fast sintering technique is regarded as a promising method to suppress grain growth because of short sintering duration [11]. The significant difference between the conventional sintering and fast sintering is the heating rate. Spark plasma sintering (SPS) method is one of the rapid sintering techniques. Some investigations showed that high heating rate had a strong limitation on the grain growth in the SPS. A large pressure is a parameter that strongly influences the final density of the materials obtained from nanometric powders. It is suggested that the combination of a fast heating rate and a large pressure is a promising mean to obtain full-density nano-grained materials.

In order to obtain a homogeneous fine-grained microstructure, the process has to start with powders of still smaller particle size, but such powders tend to agglomerate. To solve this difficulty, many advanced powders treatment methods are made to synthesize homogeneous powder mixture and keep dispersion and stabilization of nanoparticles, which are usually complex and uneconomic processes. The high price and limited sources of such a powder are not beneficial for a large-scale production of the material.

In this paper, the dense fine-grained Al_2O_3–ZrO_2 composites with submicron-nanocomposite type (alumina grain size controlled in submicron level and zirconia in nanoscale) were prepared by SPS process under large pressure. Common commercial grade

* Corresponding author. Tel.: +86 23 62408527.
E-mail address: huangweijiu@cqut.edu.cn (W. Huang).

0925-8388/$ – see front matter © 2011 Elsevier B.V. All rights reserved.
doi:10.1016/j.jallcom.2011.09.015

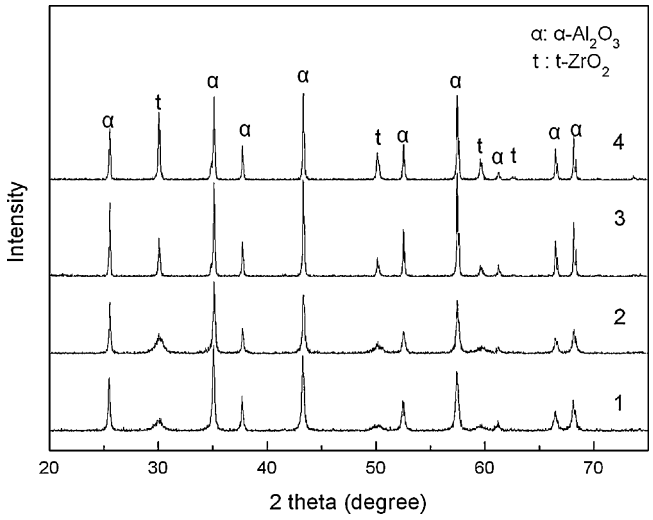

Fig. 1. X-ray diffractions of AZ5 and AZ10 powder and sintered samples: (1) sample AZ5, (2) sample AZ10, (3) sample AZ5-1400, (4) sample AZ10-1400.

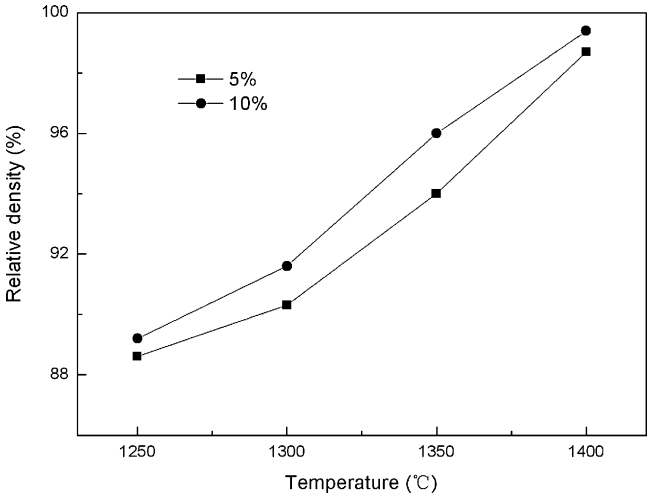

Fig. 2. Density change as a function of sintering temperature.

α-Al_2O_3 and ZrO_2 powders were used as raw materials. Mechanical mixture process (with advantages of simple process, lower cost and suitable for industry) was applied to prepare composite powder. The feasibility for the sintering of fine commercial powders without obvious grain growth was investigated. The influence of ZrO_2 content and sintering temperature on microstructures and mechanical properties of the composites were also investigated.

2. Experimental procedure

Alumina powder with an average particle size of 600 nm as the matrix phase and yttria-stabilized zirconia with 16 at% of Y_2O_3 and with a particle size of 40 nm as the dispersing phase were used as starting materials to fabricate the Al_2O_3–ZrO_2 nanocomposites, respectively. Two kinds of mixtures (5 wt% and 10 wt% ZrO_2; denoted AZ5, AZ10) were milled in ethanol by a conventional wet ball milling method for 24 h. The slurries were dried at 90 °C in an evaporator. Three grams of powders was uniaxially pressed into disks with a diameter of 2 cm and a height of 1 cm in a steel die. The disk was followed by cold isostatic pressing (CIP) at 200 MPa. The prepared disks were sintered using a SPS system (SPS 1050, Sumitomo Coal Mining Co. Ltd., Japan) in a graphite mold. The sintering temperatures were controlled at 1200–1400 °C for 2 min under 100 MPa in a vacuum atmosphere, and the heating rate was about 200 °C/min. The temperature was measured with an optical pyrometer focused on a hole in the graphite mold.

The dense samples were cut and polished. The density was measured by Archimedes method and the phase identification was characterized by anode X-ray diffraction (XRD) analyses. The microstructure was investigated via scanning electron microscope (SEM, JSM-5610LV). Grain size analysis was performed from the digitized SEM photographs using image analysis software (Nikon Image, Nikon Corporation, Japan). The Vicker's Hardness (HV) was measured by hardness testing machine (Wolpert 430SVD, USA) with 1.5 kg load and 15 s dwell time. The fracture toughness was determined by the single-edge-notched-beam (SENB) technique. The notch was generated by cutting with a diamond saw. The width of the notch was approximately 0.3 mm.

3. Results and discussions

3.1. Al_2O_3 and ZrO_2 phase evolution during sintering

In order to investigate the phase development, all the sintered AZ5 and AZ10 were examined by XRD. Fig. 1 plots the XRD patterns of both the raw powders (AZ5, AZ10) and the sintered samples at 1400 °C for 2 min (named AZ5-1400, AZ10-1400, respectively). In the raw specimen spectra, it could be found that the t-ZrO_2 peaks intensity is broad and weak and indicate the fine particle of the raw materials. In the sintered specimen spectra, there still consist of the α-alumina and t-ZrO_2 phase and no other phases are detected. But the peak characteristic of both phases becomes sharp and intense, which means the grain size of ZrO_2 increased. This result is in good agreement with what has been reported by Liu et al. [12]. In their report, Al_2O_3–ZrO_2 composites with 3–12 wt% ZrO_2 were prepared at 1500 °C and it was found higher content of ZrO_2 with the absence of yttrium stabilizer led to the presence of monoclinic phase. When the 3 mol%Y_2O_3 stabilized zirconia was used, the ZrO_2 particles are mainly of tetragonal phase. In addition to the type and amount of stabilizer, the properties and content of the starting powder also affect the transformation of tetragonal zirconia. Suffner et al. studied the microstructure evolution of metastable (ZrO_2–3 mol% Y_2O_3 + 20 wt% Al_2O_3) composite powders during spark plasma sintering at 1400 °C [13]. Phase evolution process indicates that two tetragonal phases are present in the matrix (t-ZrO_2(Y, Al) and t-ZrO_2(Y)), both with different lattice parameters.

3.2. Effect of sintering temperature on density and grain size

Fig. 2 shows the relationship of the relative density with the relative density and sintering temperature. As seen in Fig. 2, the relative density was a linear function of the sintering temperature. The relative densities increased steadily from 88 to 99% with increasing sintering temperature. Also, the results show that relatively high temperatures are required to achieve high densities. At a certain temperature, the relative density increased with the increase of ZrO_2 content. There was a little faster increase of densification for the sample with a higher ZrO_2 content at the same sintering temperature. When the temperature reached 1400 °C, the relative densities of AZ10 composites reached maximum values about 99%. This is similar to the results of the Al_2O_3–ZrO_2 composites prepared by Ye and Yang et al. [9,14]. In their results, when its percentage was less than 20 wt%, ZrO_2 nanoparticles could be uniformly dispersed in Al_2O_3 matrix. As the homogeneous dispersion of ZrO_2 nanoparticles could effectively restrain the abnormal growth of Al_2O_3 grains, ZrO_2 nanoparticles can accelerate densification of samples under this circumstance. However, when its percentage was over 20 wt%, ZrO_2 nanoparticles could not be uniformly dispersed in Al_2O_3 matrix. The inhomogeneous dispersion of ZrO_2 nanoparticles in Al_2O_3 matrix could form large pores and a high temperature is necessary to eliminate the pores and form dense bodies, which could cause the abnormal growth of Al_2O_3 grains and lead to expansion till cracking, causing the decreasing of the relative densities, strength and fracture toughness of samples. Ma et al. [15] also studied the effects of the contents of ZrO_2 on the sintering densification and microstructure of the Al_2O_3–ZrO_2. The relative density of the series samples increased with the ZrO_2

content when it was less than 15 vol%, and they reached maximum values at 15 vol%.

Spark plasma sintering of a commercially submicrometer-sized alumina powder has been studied and reported in previous papers [11]. Full-density fine-grained alumina ceramics could obtain under a pressure of 100 MPa within 3 min and 1200 °C. In comparison, the rate of densification Al_2O_3–ZrO_2 composites fabricated by the SPS is delayed with the addition of ZrO_2. With regard to nanocomposite Al_2O_3/ZrO_2, due to the adoption of fine Al_2O_3 powder and nano ZrO_2 powder, which is prone to locate in the interstices of the densified Al_2O_3 matrix, lattice diffusion and/or grain boundary diffusion which are major densification mechanisms in the high-temperature regime [16]. When ZrO_2 particles are located at grain boundaries in the intermediate and final stages of sintering, the grain boundary diffusion path becomes longer, and the diffusion of atoms/vacancies along the interface between the Al_2O_3 grain and ZrO_2 particle should decrease. The observed retardation of the densification, therefore, is thought to be due to the decrease in the grain boundary and lattice diffusivity. Therefore, in the composite case, higher temperatures for densification should be required to supplement the decrease in the diffusivity, compared with pure Al_2O_3.

At the same time, SPS is shown to be a highly efficient technique for densification of fine-grained Al_2O_3–ZrO_2 composites at temperatures 100–200 °C lower than that needed by conventional sintering. This reduction in sintering temperature is attributed to the higher pressure (100 MPa) and the efficient heat transfer from spark discharge between the particles [10]. Further, applied electric field also promotes the diffusion of ions and vacancies which enhance the sintering rate. In the case of SPS experiments, a strong macroscopic pressure is applied to the compact, so the local effective pressure can be very high when the porosity is still open. In that case, it is easy to remove the solid/vapor interfaces by rearrangement and/or grain boundary sliding and accelerate densification [17,18]. This leads to a decrease in the sintering temperature and a limitation of grain growth.

Spark plasma sintering of a commercially available zirconia powder has been investigated by Bernard-Granger et al. [18–20]. It was found that the sample obtained by SPS resides in the intragranular dislocation activity (close to zero when sintering by hot-pressing (HP) vs. very frequent in the case of SPS). The total ionic conductivity of the ZrO_2 sample sintered by HP was also 1.5–2.2 times lower than the one measured on the sample sintered by SPS [19,20]. Because dislocations are sources/sinks of vacancies, then it is understandable that a higher dislocation density will promote ionic conductivity and accelerate the grain boundary or lattice diffusion [16–19]. When the contents of ZrO_2 are higher, the diffusion of atoms/vacancies along the interface between the Al_2O_3 grain and ZrO_2 particle should increase, so the densification rate would have a little increase.

At a given sintering temperature, the grain size of the Al_2O_3 matrix with 5–10 wt% ZrO_2 differs notably, as shown in Fig. 3. The Al_2O_3 and ZrO_2 grain sizes were observed to increase with increasing sintering temperature. When the sintering temperature was given, the alumina grain size decreased with the increase of ZrO_2 content. The alumina grain size prepared from 5 wt%-ZrO_2 was larger than that obtained from 10 wt%-ZrO_2. The reasons can be explained as follows. Firstly, the presence of the second phase ZrO_2 can pin on the grain boundary and hinder grain boundary motion, which will in turn suppress the grain growth effectively. Secondly, in nanocomposite ceramics, especially in the ZrO_2 nanocomposite, the dislocation net or sub-grain boundary forms in matrix grains due to the hot stress in the cooling process [21], which results in a decrease of the matrix grain. As the ZrO_2 particles in all Al_2O_3–ZrO_2 composites have a similar grain size, the increase of ZrO_2 content increases the number of ZrO_2 particles. More ZrO_2 particles at grain

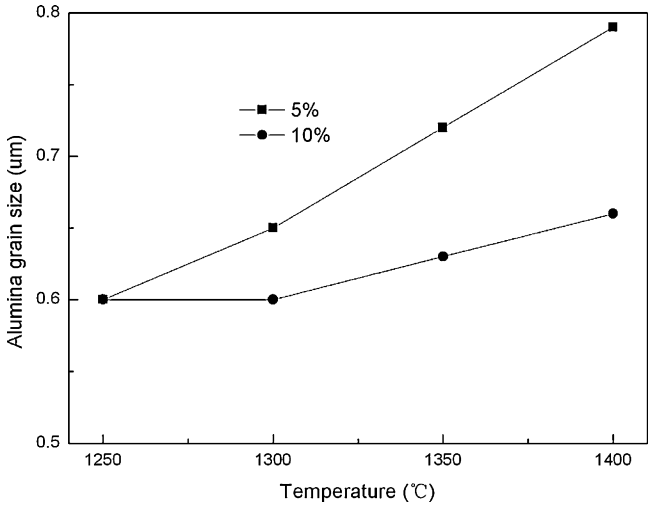

Fig. 3. Influence of sintering temperature on alumina grain size.

boundary of Al_2O_3 exert higher dragging force for the movement of grain boundary. For a composite containing nano-sized inclusions, the matrix grain size decreases with the increase of second-phase particle content [22]. Based on the theoretical analysis and experimental measurements, Tuan et al. also found that an addition of 1–2 vol% of fine zirconia particles was sufficient to prohibit the coarsening of alumina grains [22]. So the size of alumina grains is reduced with the increase of ZrO_2 content.

3.3. Microstructural behavior evolution

The microstructures of the composites observed by SEM after sintering at 1350 and 1400 °C are shown in Figs. 4 and 5. Fig. 4a demonstrates a SEM image of the polished surfaces of Al_2O_3–ZrO_2 composites containing 5 wt% ZrO_2, and b is the content of 10 wt%. As shown in Fig. 4a and b, pores between Al_2O_3 particles were clearly found and the microstructure was not dense. This result is in agreement with the relative density data given in Fig. 2. It also implies that 1350 °C is not enough to obtain the full-dense sample. It was found that the grain sizes of Al_2O_3 had no obvious increase, while that of ZrO_2 had a slight increase. The SEM examination in Fig. 5a and b confirms that the sample sintered at temperature of 1400 °C results in a significant change in microstructure, and both samples clearly exhibited homogeneous and dense microstructure. As can be seen, the smaller zirconia grains were homogeneously dispersed in the alumina matrix. The grain sizes of Al_2O_3 were observed to decrease with increasing ZrO_2 content from 5 to 10 wt%. For AZ5 the mean grain size of alumina was around 0.8 μm, while for the sample AZ10 the mean grain size decreased to 0.65 μm. The grain sizes of ZrO_2 were observed to increase with increasing ZrO_2 content, and the average grain size was about 150 nm. In addition, some larger ZrO_2 grains with a size of 400–500 nm was obtained in AZ10 sample. A limited amount of zirconia grains were located at the boundaries of alumina grains, and most of them are in present at triple junctions, resulting in an intergranular type nanocomposite.

3.4. Relationship between microstructure and mechanical properties

The variation of the Vickers microhardness of the prepared Al_2O_3–ZrO_2 samples with the ZrO_2 content is shown in Fig. 6 (samples AZ5-1400 and AZ10-1400). The Vickers microhardness increased with increasing ZrO_2 content. AZ10 measured with 1 kg load had Vickers microhardness as high as 20 GPa, and with 5 kg

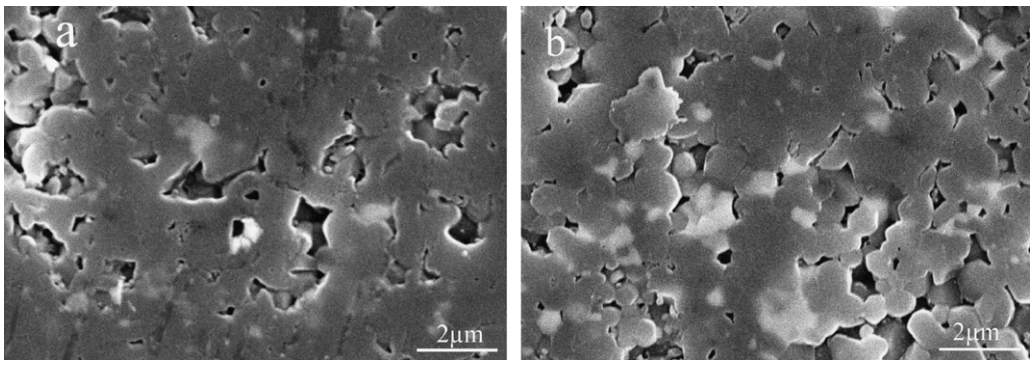

Fig. 4. Scanning electron microscopy micrographs of the thermally etched surfaces of Al_2O_3–ZrO_2 samples, sintered by SPS at 1350 °C, (a) 5%; (b) 10%.

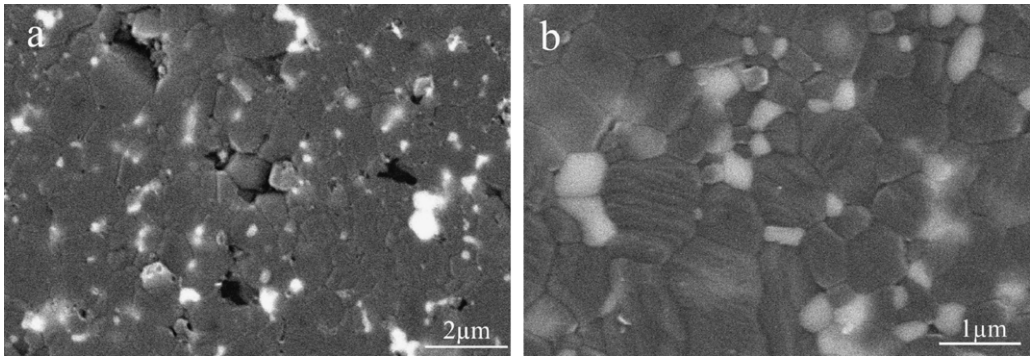

Fig. 5. Scanning electron microscopy micrographs of the thermally etched surfaces of Al_2O_3–ZrO_2 samples, sintered by SPS at 1400 °C, (a) 5%; (b)10%.

load had Vickers microhardness over 18 GPa. Usually, the Vickers microhardness of the Al_2O_3–ZrO_2 ceramics with micro-nano structure is 14–15 GPa [23], whereas the sample with submicro-nano structure have a higher microhardness in our present work. This is mostly attributed to the submicro-nano structure and high density of the sample AZ10. According to Hall-Petch formula, the fine grains will result in an increase of the microhardness. The fracture toughness value of AZ5 and AZ10 were 4.5 and 5.1 MPa $m^{1/2}$, respectively. Previous literatures [11,24] have reported fracture toughness of sintered pure alumina with sub-micron grain size. The full-dense specimens sintered by HIP presented a grain size of 0.45 μm and fracture toughness of K_{IC} = 3.5 MPa $m^{1/2}$ [24]. The submicron-grained Al_2O_3 sintered by SPS had a fracture toughness value of 3.8 MPa $m^{1/2}$ [11]. It has been shown that the presence of zirconia particles results in an improved toughness than pure Al_2O_3. At the same time, the fracture toughness of the composites increased with increasing volume fraction of ZrO_2. Similar results of fracture toughness were also observed in the ZrO_2–Al_2O_3 composites with a fine-grained structure [7]. The composite (7.5 vol% ZrO_2) obtained by the colloidal processing presented a fine structure (Al_2O_3 grain size: 1.1 μm, ZrO_2 grain size: 0.4 μm) and a fracture toughness value of 5.3 MPa $m^{1/2}$. The toughness enhancement for all the composites investigated in the present study can be attributed to a transformation toughening effect. In a ceramic containing a suitable distribution of metastable t-ZrO_2, the stress-activated t → m transformation in the stress field of a potentially damaging crack imparts useful toughness to the ceramic through mechanisms associated with the accommodation of the transformation shape change. The volume change accompanying transformation creates a compressive strain field about the crack tip to oppose crack propagation [25]. A larger amount of tetragonal zirconia grains in the alumina matrix will cause more phase transformation participating in the fracture process, so the toughness could increase linearly with the amount of transformable zirconia [5,26]. At the same time, with the refinement of microstructure, the residual strains after cooling will further improve the resistance to crack propagation [27]. The contribution of crack deflection could be another reason for this improvement. With decreasing in grain size, the number of grains per area was increased and causing a larger degree of crack deflection by the grain boundaries [28]. Since the zirconia grains are initially stabilized by yttria, the monoclinic phase is not be detected by XRD in the sintered samples. It means that there is no microcrack (result from t → m transformation) present during cooling from sintering; therefore the contribution from microcracking toughening mechanisms is small.

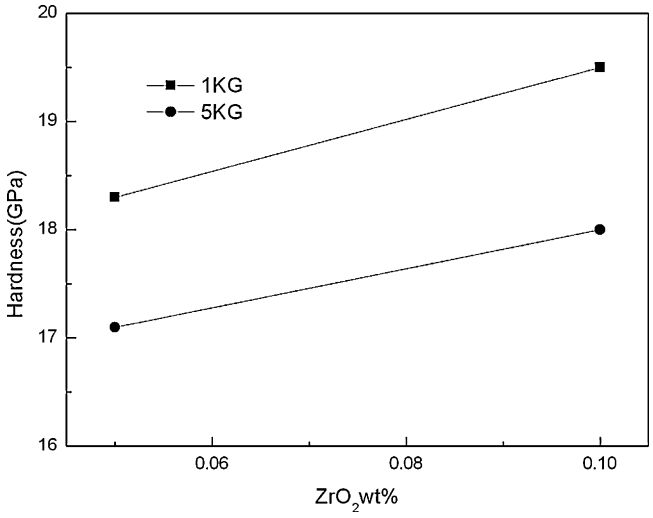

Fig. 6. Relationship between the Vickers microhardness and ZrO_2 content.

4. Conclusions

Fine-grained Al_2O_3–ZrO_2 composites with different ZrO_2 content were prepared by the SPS method. Near theoretical densities were obtained at a low sintering temperatures of 1400 °C with a holding time of 2 min and pressure of 100 MPa. The grain size of alumina decreased with the increase of ZrO_2 content. The ZrO_2 grain sizes were observed to increase with increasing ZrO_2 content. Compared with the size of raw materials, microstructure analysis indicated that the alumina grains had no significant growth. The sample with 10 wt% ZrO_2 content has the maximum density, and the mean grain sizes of ZrO_2 and Al_2O_3 were 150 and 650 nm, respectively. The Vickers microhardness and fracture toughness increased with increasing ZrO_2 content and the highest value reached 18 GPa (5 kg load) and 5.1 MPa $m^{1/2}$, respectively.

Acknowledgements

This work was financially supported by National Natural Science Foundation of China (50975302, 51102289), the Natural Science Foundation Project of CQ (CSTC2009BB4385) and Chongqing Key Science Foundation of Chongqing Science and Technology Commission (CSTC, 2008BA4037).

References

[1] K. Niihara, J. Ceram. Soc. Jpn. 99 (10) (1991) 974–982.
[2] A.H. De Aza, J. Chevalier, G. Fantozzi, M. Schehl, R. Torrecillas, Biomaterials 23 (2002) 937–945.
[3] A. Okada, J. Eur. Ceram. Soc. 28 (2008) 1097–1104.
[4] C.J. Wang, C.Y. Huang, Y.C. Wu, Ceram. Int. 35 (2009) 1467–1472.
[5] W.H. Tuan, R.Z. Chen, T.C. Wang, C.H. Cheng, P.S. Kuo, J. Eur. Ceram. Soc. 22 (2002) 2827–2833.
[6] J.R. Kelly, I. Denry, Dent. Mater. 24 (2008) 289–298.
[7] A.H. De Aza, J. Chevalier, G. Fantozzi, J. Am. Ceram. Soc. 86 (1) (2003) 115–120.
[8] F.A.T. Guimaraes, K.L. Silva, V. Trombini, J.J. Pierri, J.A. Rodrigues, R. Tomasi, E.M.J.A. Pallone, Ceram. Int. 35 (2009) 741–745.
[9] Y.P. Ye, J.G. Li, H.D. Zhou, J.M. Chen, Ceram. Int. 34 (2008) 1797–1803.
[10] Z.A. Munir, U. Anselmi-Tamburini, M. Ohyanagi, J. Mater. Sci. 41 (2006) 763–777.
[11] Z. Shen, M. Johnsson, Z. Zhao, M. Nygren, J. Am. Ceram. Soc. 85 (2002) 1921–1927.
[12] G.W. Liu, Z.P. Xie, Y. Wu, Mater. Des. 32 (2011) 3440–3447.
[13] J. Suffner, M. Lattemann, H. Hahn, L. Giebeler, C. Hess, I.G. Cano, S. Dosta, J.M. Guilemany, C. Musa, A.M. Locci, R. Licheri, R. Orru, G. Cao, J. Am. Ceram. Soc. 93 (9) (2010) 2864–2870.
[14] G. Yang, J.C. Li, G.C. Wang, M. Yashima, S.L. Min, J. Mater. Sci. 40 (2005) 6087–6090.
[15] W.M. Ma, L. Wen, R.G. Guan, X.D. Sun, X.K. Li, Mater. Sci. Eng. A 477 (2008) 100–106.
[16] G.J. Liu, H.B. Qiu, R. Todd, R.J. Brook, J.K. Guo, Mater. Res. Bull. 33 (2) (1998) 281–288.
[17] J.H. Chae, K.H. Kim, Y.H. Choa, J. Matsushita, J.W. Yoon, K.B. Shim, J. Alloys Compd. 413 (2006) 259–264.
[18] G. Bernard-Granger, C. Guizard, Acta Mater. 55 (2007) 3493–3504.
[19] G. Bernard-Granger, C. Guizard, S. Surble, G. Baldinozzi, A. Addad, Acta Mater. 56 (2008) 4658–4672.
[20] G. Bernard-Granger, A. Addad, G. Fantozzi, G. Bonnefont, C. Guizard, D. Vernat, Acta Mater. 58 (2010) 3390–3399.
[21] M. Sternitzke, J. Eur. Ceram. Soc. 17 (9) (1997) 1061–1082.
[22] W.H. Tuan, J.R. Chen, C.J. Ho, Ceram. Int. 34 (2008) 2129–2135.
[23] J.H. Gong, H.Z. Miao, B.J. Hu, Mater. Sci. Eng. A 372 (2004) 207–212.
[24] J. Echeberriaa, J. Tarazonnaa, J.Y. Heb, T. Butlerb, F. Castroa, J. Eur. Ceram. Soc. 22 (2002) 1801–1809.
[25] R.H.J. Hannink, P.M. Kelly, B.C. Muddle, J. Am. Ceram. Soc. 83 (3) (2000) 461–487.
[26] A. Nevarez-Rascon, A. Aguilar-Elguezabal, E. Orrantia, M.H. Bocanegra-Bernal, Int. J. Refract. Met. Hard Mater. 27 (2009) 962–970.
[27] V. Sergo, G. Pezzotti, O. Sbaizero, T. Nishida, Acta Mater. 46 (5) (1998) 1701–1710.
[28] C. Santos, M.H. Koizumi, J.K.M.F. Daguanoa, F.A. Santosa, C.N. Elias, A.S. Ramos, Mater. Sci. Eng. A 502 (2009) 6–12.